The Plant Cell, Vol. 25: 2878–2891, August 2013, www.plantcell.org

Arabidopsis Histone Methylase CAU1/PRMT5/SKB1 Acts as an Epigenetic Suppressor of the Calcium Signaling Gene *CAS* to Mediate Stomatal Closure in Response to Extracellular Calcium[W]

Yan-Lei Fu, Guo-Bin Zhang, Xin-Fang Lv, Yuan Guan, Hong-Ying Yi, and Ji-Ming Gong[1]

National Key Laboratory of Plant Molecular Genetics and National Center for Plant Gene Research (Shanghai), Institute of Plant Physiology and Ecology, Shanghai Institutes for Biological Sciences, Chinese Academy of Sciences, Shanghai 200032, People's Republic of China

ORCID ID: 0000-0003-2105-0587 (J-M.G).

Elevations in extracellular calcium ($[Ca^{2+}]_o$) are known to stimulate cytosolic calcium ($[Ca^{2+}]_{cyt}$) oscillations to close stomata. However, the underlying mechanisms regulating this process remain largely to be determined. Here, through the functional characterization of the calcium underaccumulation mutant *cau1*, we report that the epigenetic regulation of CAS, a putative Ca^{2+} binding protein proposed to be an external Ca^{2+} sensor, is involved in this process. *cau1* mutant plants display increased drought tolerance and stomatal closure. A mutation in *CAU1* significantly increased the expression level of the calcium signaling gene *CAS*, and functional disruption of CAS abolished the enhanced drought tolerance and stomatal $[Ca^{2+}]_o$ signaling in *cau1*. Map-based cloning revealed that *CAU1* encodes the H4R3sme2 (for histone H4 Arg 3 with symmetric dimethylation)-type histone methylase protein arginine methytransferase5/Shk1 binding protein1. Chromatin immunoprecipitation assays showed that CAU1 binds to the *CAS* promoter and modulates the H4R3sme2-type histone methylation of the *CAS* chromatin. When exposed to elevated $[Ca^{2+}]_o$, the protein levels of CAU1 decreased and less CAU1 bound to the *CAS* promoter. In addition, the methylation level of H4R3sme2 decreased in the *CAS* chromatin. Together, these data suggest that in response to increases in $[Ca^{2+}]_o$, fewer CAU1 protein molecules bind to the *CAS* promoter, leading to decreased H4R3sme2 methylation and consequent derepression of the expression of *CAS* to mediate stomatal closure and drought tolerance.

INTRODUCTION

Cytosolic calcium ($[Ca^{2+}]_{cyt}$) plays a pivotal role as a second messenger in plant development and interactions with the environment (Helpler and Wayne, 1985; Poovaiah and Reddy, 1993; Bush, 1995). Various signals, including biotic stress, abiotic stress, hormones, and mechanical disturbance, are sensed by plant cells and elicit repetitive oscillation or spiking of $[Ca^{2+}]_{cyt}$, which are termed Ca^{2+} signatures and regulated by Ca^{2+} channels, pumps, or carriers localized at the plasma membrane or in the membranes of organelles (Bush, 1995; Thuleau et al., 1998; Rudd and Franklin-Tong, 1999; Sanders et al., 1999; Allen et al., 2000, 2001; Harper, 2001). These Ca^{2+} signatures vary in frequency and amplitude in response to different stimuli and thus are believed to encode stimulus-specific information that can be transduced and sensed by downstream Ca^{2+} sensors, including calmodulins, calcium-dependent proteins, and calcineurin B-like proteins (Zielinski, 1998; Luan et al., 2002; Sanders et al., 2002). These calcium sensors decode Ca^{2+} signatures by binding Ca^{2+} ions via conserved EF-hand domains and transduce them into specific cellular responses, such as altered phosphorylation and expression of target genes, to bring about physiological responses corresponding to the original stimuli (Luan et al., 2002; Sanders et al., 2002).

In contrast with intracellular Ca^{2+}, the role of extracellular Ca^{2+} ($[Ca^{2+}]_o$) remains to be determined. In mammals and other animals, parathyroid cells can alter the secretion of parathyroid hormone in response to serum Ca^{2+} levels, which in turn modulates Ca^{2+} uptake from the intestine, net release from the skeleton and its conservation efficiency in the kidneys, thus returning serum Ca^{2+} to a baseline level (Shoback et al., 1983, 1984; Brown, 1991). It was later proposed that Ca^{2+} can actually serve as an extracellular first messenger (Brown, 1991), as parathyroid gland cells are able to sense $[Ca^{2+}]_o$ levels in the serum and produce intracellular Ca^{2+} signals through the activation of CaR, a G protein–coupled Ca^{2+}-sensing receptor, and the phospholipase C/inositol-1,4,5-trisphosphate (IP3)/Ca^{2+} signaling pathway (Brown et al., 1987, 1993; Shoback et al., 1988).

In plants, evidence indicating a similar function for $[Ca^{2+}]_o$ has been mainly provided by studies of stomatal guard cells (Schwartz, 1985; MacRobbie, 1992; Allen et al., 2000, 2001; Han et al., 2003). When exposed to $[Ca^{2+}]_o$, $[Ca^{2+}]_{cyt}$ oscillation was observed in guard cells, and the oscillation patterns varied with different extracellular Ca^{2+} levels (McAinsh et al., 1995; Allen et al., 2000). Abortion or alteration in $[Ca^{2+}]_{cyt}$ oscillations failed to induce stomatal closure in response to $[Ca^{2+}]_o$ (Allen et al., 2000, 2001). These observations suggested that $[Ca^{2+}]_o$ signals can be perceived by cells and are encoded in the intracellular Ca^{2+} signatures. The isolation of CAS and identification of its downstream signaling components provided further evidence for this hypothesis

[1] Address correspondence to jmgong@sibs.ac.cn.
The author responsible for distribution of materials integral to the findings presented in this article in accordance with the policy described in the Instructions for Authors (www.plantcell.org) is: Ji-Ming Gong (jmgong@sibs.ac.cn).
[W] Online version contains Web-only data.
www.plantcell.org/cgi/doi/10.1105/tpc.113.113886

(Han et al., 2003; Hetherington and Brownlee, 2004; Tang et al., 2007, Wang et al., 2012a). However, given that CAS localizes exclusively to chloroplasts instead of the cell surface, where $[Ca^{2+}]_o$ sensing is supposed to occur (Nomura et al., 2008; Vainonen et al., 2008; Weinl et al., 2008), we postulate that other regulatory components must exist upstream of *CAS* if the hypothesis should stand.

In this study, a Ca^{2+} underaccumulation mutant, *cau1*, was identified in a large-scale genetic screen. The mutant showed enhanced stomatal closure and drought tolerance. Further analysis showed that *CAU1* encodes an H4R3sme2-type histone methylase and acts as an immediate upstream suppressor of the *CAS* gene. Elevated $[Ca^{2+}]_o$ decreases CAU1 protein levels and consequently the H4R3sme2 methylation level in the *CAS* chromatin, thus derepressing *CAS* expression to close stomata.

RESULTS

Isolation and Characterization of the Calcium Underaccumulation Mutant *cau1*

In a large-scale screen of Ca^{2+} accumulation mutants, a Ca^{2+} underaccumulation mutant, *cau1*, was identified (Figure 1A). Compared with the wild type Columbia-0 (Col-0), *cau1* plants accumulated less Ca^{2+} and Fe in rosette leaves, but their copper and $zinc^{2+}$ accumulation was significantly increased (Figure 1A). Further analysis showed that Ca^{2+} accumulation was decreased in the shoots of *cau1* when treated with 0.5 mM Ca^{2+} (see Supplemental Figure 1A online). These results demonstrated that *CAU1* preferentially regulates Ca^{2+} accumulation in the aerial parts.

Interestingly, enhanced drought tolerance was also observed to cosegregate with the ionomic phenotype of *cau1*. When exposed to drought stress, Col-0 was severely dehydrated and did not recover upon reirrigation. By contrast, *cau1* did not show any significant dehydration after 9 d of drought treatment and was able to fully recover from 10 or 12 d of drought (Figure 1B). Other visual phenotypes, including partial and degenerate chlorosis in young leaves, increased lateral shoots with as many as 10 cauline leaves, and late flowering, were also observed in *cau1* mutant plants (see Supplemental Figure 2 online).

As Ca^{2+} accumulation fluctuates with plant ages, and *cau1* mutant plants were late flowering, we further analyzed the Ca^{2+} levels from plants of different ages. As expected, Ca^{2+} accumulation did vary from 21 to 50 d of age, though overall significantly lower Ca^{2+} levels were detected in *cau1* compared with Col-0 at all analyzed ages (see Supplemental Figure 1B online). The Ca^{2+} levels in *cau1* were also consistently lower than those of RRS-7 and Lov-1, which were randomly selected as representative late-flowering ecotypes (see Supplemental Figure 1C online) and later found to show no changes in *CAS* expression (see Supplemental Figure 1D online). These results suggested that *CAU1* functions to regulate ion homeostasis and plant development independently.

Genetic Analysis of the *cau1* Mutant and Map-Based Cloning of the *CAU1* Gene

After backcrossing the homozygous *cau1* to Col-0, a phenotypic assay was performed in the derived F1 and F2 generations. All F1 progenies grew and developed similarly to the wild type. In the F2 generation, the segregation of 221 wild-type plants and 75 *cau1* mutant corresponded to the expected ratio of 3:1 ($\chi^2 = 0.018$, $P = 0.893$), indicating that *cau1* carries a single recessive mutation.

To isolate the mutant gene, *cau1* was outcrossed to the ecotype Landsberg *erecta* and the F1 progenies were self-pollinated to generate an F2 mapping population. Bulked segregant analysis using 198 F2 mutants roughly mapped the *cau1* locus to the distal arm of chromosome 4, between the simple sequence length polymorphism (SSLP) markers NGA8 and NGA1107 (Figure 2A). Fine mapping using 5742 F2 mutant plants further localized the *cau1* locus to a 43-kb genomic region between markers F6I18 and F6E21 (Figure 2A). Fifteen genes were predicted in this region, and sequencing of these candidate genes revealed a G nucleotide deletion in the third exon of the At4g31120 locus (Figure 2B), which resulted in a shift of the open reading frame and, hence, a premature stop codon 40 bp downstream of the mutation site. A complementation assay using the coding sequence of the At4g31120 locus successfully restored drought tolerance (Figure 2C), ion accumulation (see Supplemental Figure 3A online), and morphological alteration (see Supplemental Figures 3C to 3F online) to wild-type levels. RT-PCR further showed that the mRNA level of At4g31120 was decreased in *cau1* (see Supplemental Figure 3B online).

At4g31120 was previously identified as *PRMT5/SKB1* (Pei et al., 2007; Wang et al., 2007), and we analyzed drought tolerance and ion accumulation in the T-DNA insertion mutant line *skb1-2* (Salk_095085). As expected, comparable phenotypes for both drought tolerance (Figure 2C) and Ca^{2+} underaccumulation (Figure 2D) were observed in the *cau1* and *skb1-2* mutant lines. These data demonstrated that the mutation in At4g31120 is responsible for the observed *cau1* phenotypes.

CAS Expression Is Steadily Elevated in the *cau1* Mutant

CAU1/PRMT5/SKB1 has been identified as a type II methyltransferase, regulating pleiotropic physiological processes by either H4R3sme2 regulation and/or pre-mRNA splicing (Pei et al., 2007; Wang et al., 2007; Schmitz et al., 2008; Deng et al., 2010; Hong et al., 2010; Sanchez et al., 2010; Zhang et al., 2011). To investigate how CAU1 regulates Ca^{2+} level and drought tolerance, microarray analyses were performed. Among the genes with significantly altered expression, *FLC* was upregulated in *cau1* (see Supplemental Table 1 online), an observation that is consistent with the late flowering phenotype observed in this (see Supplemental Figures 2D to 2F online) and previous studies (Wang et al., 2007).

More significantly, the expression of *CAS* was enhanced in *cau1* compared with the wild-type Col-0 (see Supplemental Table 1 online). Given that CAS mediates $[Ca^{2+}]_o$ signaling (Han et al., 2003; Tang et al., 2007; Nomura et al., 2008; Weinl et al., 2008) and Ca^{2+} levels were altered in *cau1*, we performed quantitative RT-PCR and found that upon exposure to increased external Ca^{2+} concentrations, the expression levels of *CAS* were upregulated in the wild-type Col-0, in contrast with the constitutively high levels in the mutants *cau1* and *skb1-2* (Figure 3A). Note that Ca^{2+} treatments did not significantly affect *CAU1* expression (Figure 3B).

In addition, histochemical analyses showed that β-glucuronidase (GUS) activity driven by the *CAS* promoter was higher in *cau1*

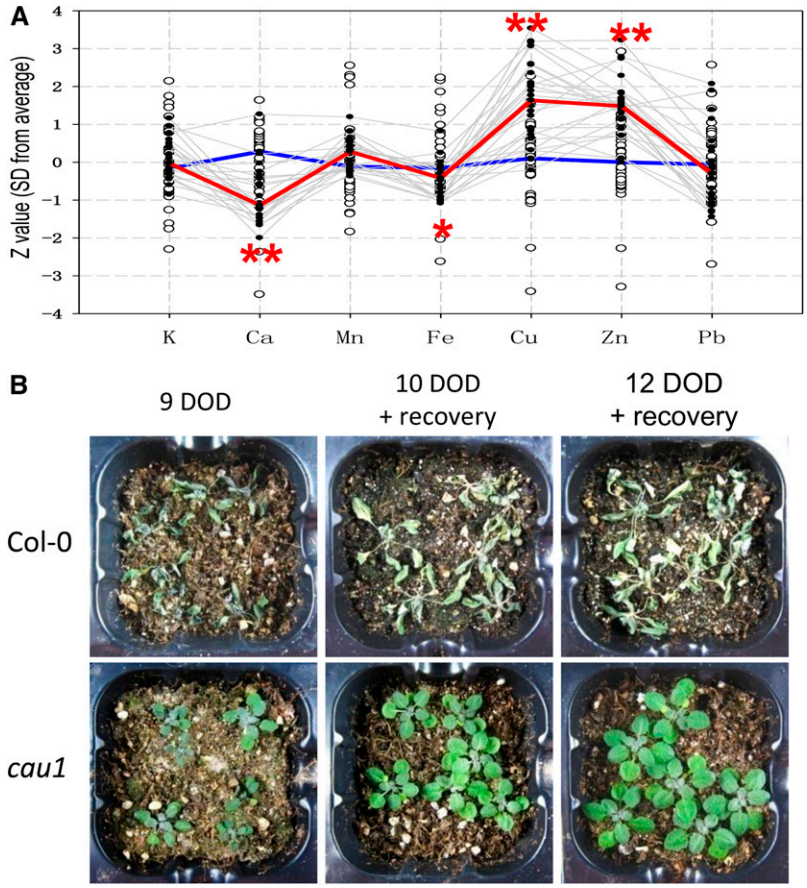

Figure 1. The Calcium Underaccumulation Mutant *cau1* with Enhanced Drought Tolerance.

(A) Ion accumulation profile of *cau1*. Seven cationic elements in *cau1* M3 mutant plants were measured by ICP-MS. Open black circles represent *Z* values (SD from the average value of the wild type control, *y* axis) of the individual wild-type controls, and gray lines highlight the ion profile data of *cau1* mutants. Median *Z* values of the wild type ($n > 30$) and *cau1* mutants ($n > 30$) were calculated, and the resultant ion profiles were outlined by the blue line and red line, respectively.

(B) Wild-type and *cau1* mutant plants subjected to drought stress for 9 to 12 d. Plants were exposed to 9 d of drought (DOD) treatment or treated for 10 or 12 d and subsequently reirrigated and allowed to recover for 1 week. *P < 0.05 and **P < 0.01.

compared with Col-0 at both seedling (Figures 3D versus 3C) and mature stages (Figure 3F versus 3E). RT-PCR analysis further revealed that although *CAS* levels fluctuated in Col-0 at 21, 28, and 38 d of age, a steadily enhanced expression was observed in *cau1* (Figure 3G). *CAS* expression was restored to wild-type levels in the complemented lines (see Supplemental Figure 4G online). Taken together, these results indicate that regardless of the external Ca^{2+} levels or plant age, *CAS* expression was consistently higher in *cau1*.

In addition to *CAS* and *FLC*, several genes involved in iron uptake and metabolism were also upregulated in *cau1* (see Supplemental Table 1 online), which might explain the chlorosis observed in young leaves (see Supplemental Figures 2A to 2C, 2G, and 2H online) and the iron underaccumulation phenotype (Figure 1A).

CAU1 Mediates Drought Tolerance and Stomatal Closure through CAS

CAS has been shown to mediate $[Ca^{2+}]_o$ signaling in guard cells. Given that the Ca^{2+} underaccumulation mutant *cau1* is drought tolerant and shows constitutively enhanced *CAS* expression, we sought to determine whether these phenotypes are genetically correlated with *CAS*. The results showed that Col-0 (Figures 4A and 4E) and *cas-1* (Figures 4C and 4E) are sensitive to drought stress. By contrast, significant tolerance was observed in *cau1* plants (Figures 4B and 4E). However, in the double mutant *cau1 cas-1* plants (Figures 4D and 4E), which show growth rates similar to *cau1*, drought tolerance conferred by the *cau1* mutation was abolished. A similar phenotype was observed in the complementation line 35S/*CAU1-cau1* (see Supplemental Figures 4A to 4D online). These results indicated that *CAS* is genetically downstream of *CAU1* in mediating drought tolerance.

Stomatal apertures were also determined using fresh epidermis peeled directly from leaves. As shown in Figure 4F, increased stomatal closure was observed in *cau1* compared with Col-0, while *cas-1* and Col-0 showed similar stomatal apertures. In the double mutant *cau1 cas-1*, stomatal apertures were comparable to those of the wild type and *cas-1* mutants (Figure 4F). A previous study showed that overexpression of *CAS* led to

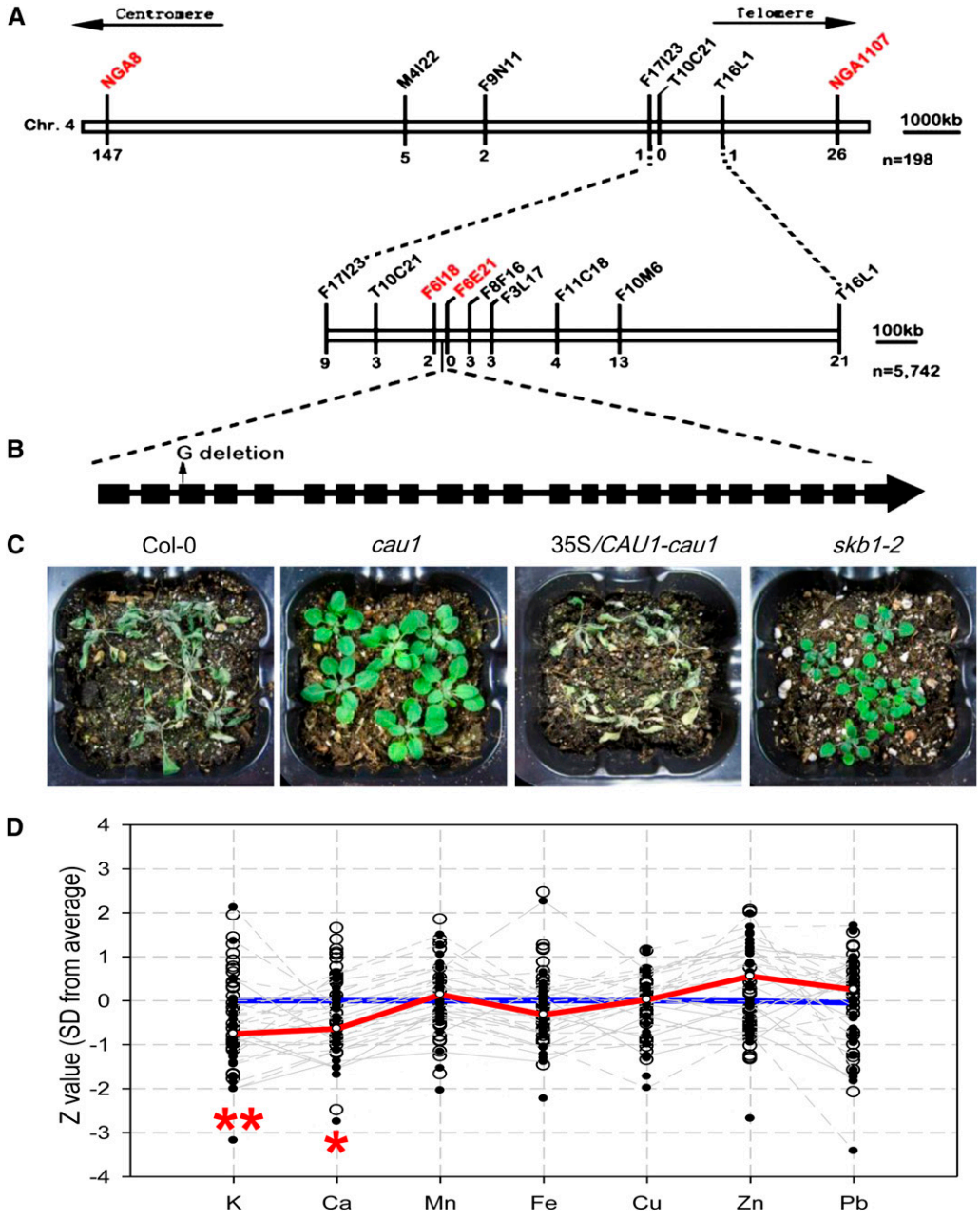

Figure 2. Molecular Identification of the *cau1* Gene.

(A) Map-based cloning of the *cau1* locus on chromosome 4.

(B) Structure of the *CAU1* gene and the mutation in the *cau1* allele. Black boxes represent exons, and black lines represent introns. The Arabidopsis Genome Initiative number for *CAU1* is At4g31120.

(C) Complementation assay of drought tolerance in *cau1*. Wild-type, *cau1* mutant, *35S/CAU1-cau1* (*cau1* harboring construct 35S/*CAU1*-pBI121), and *skb1-2* plants were subjected to dehydration for 12 d, reirrigation, and recovery for 1 week.

(D) Ion accumulation profile of *skb1-2*. Seven cationic elements in *skb1-2* mutant plants were measured by ICP-MS. Open black circles represent *Z* values (*y* axis) of individual wild-type controls, and gray lines highlight ion profiles of *skb1-2* individuals. Median *Z* values of the wild type ($n > 30$) and *skb1-2* mutant ($n > 30$) were calculated, and the consequent ion profiles were outlined by the blue line and the red line, respectively. *P < 0.05 and **P < 0.01.

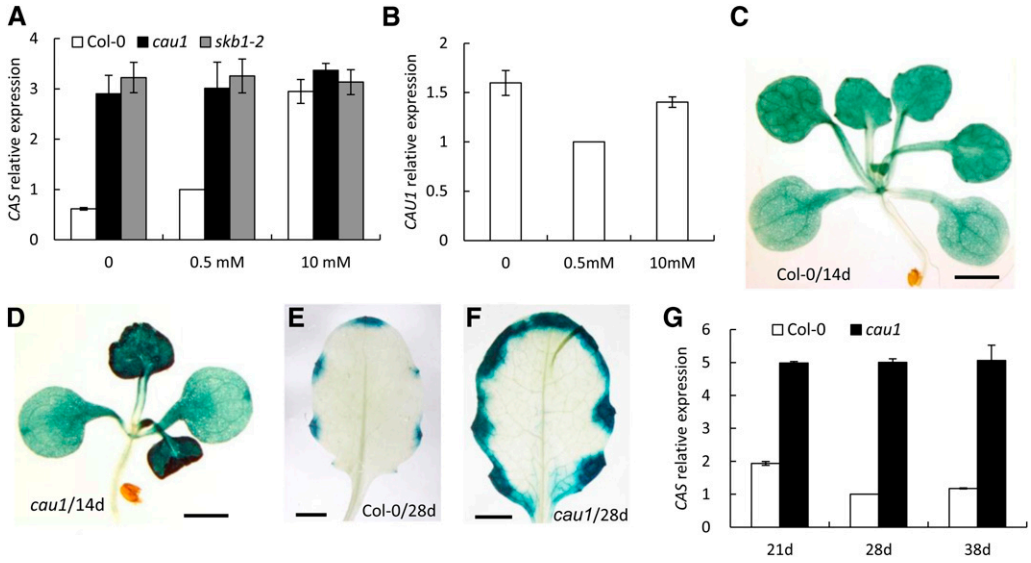

Figure 3. *CAS* Expression Is Enhanced in *cau1* Plants.

(A) and **(B)** Three-week-old plants grown hydroponically were treated with 0, 0.5, and 10 mM Ca^{2+} for 4 d. The expression levels of *CAS* **(A)** or *CAU1* **(B)** in shoots were determined by RT-PCR. *Actin2* was used as an internal control. Values are mean ± SE, $n = 3$.
(C) to **(F)** Histochemical localization of GUS driven by the *CAS* promoter in 14-d-old wild-type **(C)** and *cau1* mutant seedlings **(D)** or 28-d-old wild-type **(E)** and *cau1* leaves **(F)**. Bars = 0.25 cm.
(G) *CAS* expression in wild-type and *cau1* plants grown in soil to the indicated ages.

increased stomatal closure (Nomura et al., 2008), equivalent to the phenotype observed in *cau1*. The water loss rate was consistently increased in the *cas-1* mutant and decreased in *cau1* (Figure 4G). Crossing *cas-1* to *cau1* successfully restored the water loss rate to levels comparable to those of the wild type (Figure 4G). In the complementation line 35S/*CAU1-cau1*, both the stomatal aperture and water loss rate were restored to wild-type levels (see Supplemental Figures 4E and 4F online). These results suggest that CAS provides an essential contribution to the observed increased stomatal closure and the consequent drought tolerance and acts genetically downstream of *CAU1*. Water loss rates in the *cau1 cas-1* double mutant were not as high as in the *cas-1* mutant. CAU1 may function pleiotropically (see Supplemental Figure 2 online); thus, components other than CAS might also be involved in the control of water loss.

CAU1 Is an Upstream Regulator of the CAS-Mediated $[Ca^{2+}]_o$ Signaling in Guard Cells

To further determine whether CAU1 regulates the $[Ca^{2+}]_o$ signaling in guard cells, a stomatal closure assay was performed. As expected, apparent stomatal closure was triggered by $[Ca^{2+}]_o$ in the wild-type Col-0 and *cau1* mutant and disrupted in *cas-1* and the double mutant *cau1 cas-1* where CAS is functionally disrupted (Figure 5A). Interestingly, the starting stomatal apertures prior to $[Ca^{2+}]_o$ application were much smaller in *cau1* than in Col-0, implying that *cau1* guard cells might be oversensitive to extracellular Ca^{2+}. To test this hypothesis, EGTA was added to the opening buffer to chelate the trace amount of free Ca^{2+}. Stomatal apertures in Col-0 and *cau1* were comparable in the absence of extracellular Ca^{2+}, and upon exposure to 0.1 to 5 μM Ca^{2+}, significant stomatal closure was observed in *cau1* but not in Col-0, *cas-1*, or *cau1 cas-1* (Figure 5B). The stomatal apertures of *cau1* were restored in the complementation assay (see Supplemental Figures 5A and 5B online). Taking into account that *CAS* expression levels were consistently higher in *cau1* compared with the wild type (Figure 3), we concluded that enhanced *CAS* expression led to the increased $[Ca^{2+}]_o$ sensitivity observed in *cau1* and that CAU1 is an upstream regulator of the CAS-mediated $[Ca^{2+}]_o$ signaling in guard cells.

Consistent with this, $[Ca^{2+}]_{cyt}$ was significantly increased in *cau1* guard cells compared with the wild-type Col-0, while in *cas-1*, the level was ~50% lower than in *cau1* and significantly lower than in Col-0 (Figures 5C and 5D). In the double mutant *cau1 cas-1*, $[Ca^{2+}]_{cyt}$ levels were significantly lower than in *cau1* and comparable to *cas-1* (Figures 5C and 5D), consistent with the model proposed for CAS (Han et al., 2003; Tang et al., 2007; Nomura et al., 2008; Weinl et al., 2008). $[Ca^{2+}]_{cyt}$ was restored to wild-type levels in the *cau1* complemented lines (see Supplemental Figures 5C and 5D online). Further analysis showed that 4 d of Ca^{2+} starvation resulted in significant necrotic lesions, a typical symptom indicating plant Ca^{2+} deficiency, in *cau1* leaves (Figure 5F, indicated by red arrows), but not in Col-0 (Figure 5E), *cas-1* (Figure 5G), or the double mutant *cau1 cas-1* (Figure 5H), indicating that the increased sensitivity to Ca^{2+} starvation in *cau1* was essentially attributable to elevated *CAS* expression.

Taken together, these results (Figures 1A and 5A to 5H) demonstrated that the mutation in *CAU1* derepressed *CAS* expression, thus enhancing CAS-mediated $[Ca^{2+}]_o$ signaling and

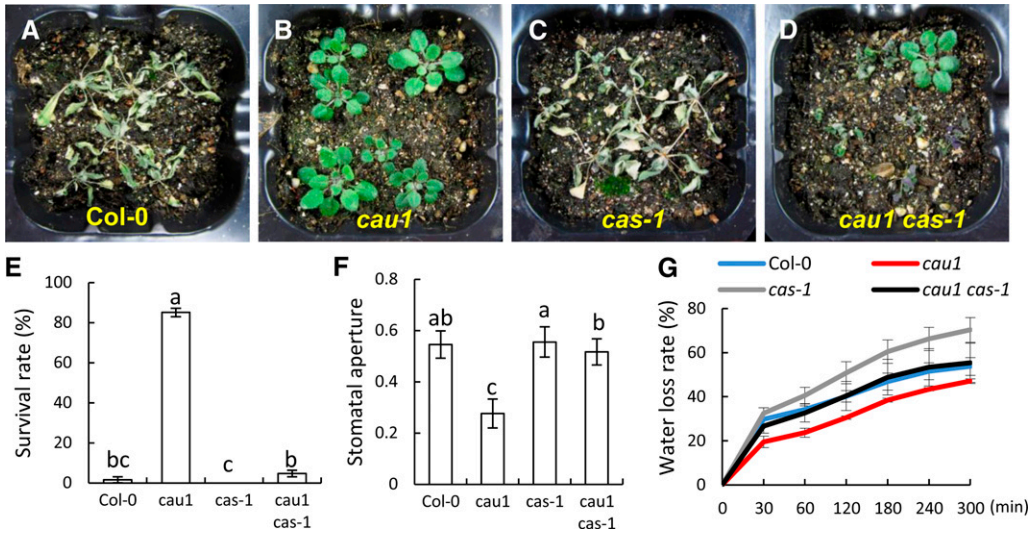

Figure 4. Increased Drought Tolerance and Stomatal Closure in *cau1* Is Attributed to *CAS*.

(A) to **(D)** Drought tolerance in wild-type **(A)**, *cau1* **(B)**, *cas-1* **(C)**, and *cau1 cas-1* **(D)** plants. Watering of 14-d-old plants was withheld for 12 d, and then plants were rewatered and allowed to recover for 1 week.

(E) Survival rates of plants exposed to drought stress in **(A)** to **(D)**. Values are mean ± SD from three independent experiments.

(F) Stomatal assay of epidermis peeled directly from 22-d-old rosette leaves. Stomatal apertures were evaluated by stomata width/length. Values are mean ± SD ($n \geq 30$). Different lowercase letters above the bars in **(E)** and **(F)** indicate statistically different averages at $P < 0.05$ in *t* tests.

(G) Water loss rate of 22-d-old wild-type, *cau1*, *cas-1*, and *cau1 cas-1* plants. Values are mean ± SD calculated from three independent experiments, each containing data from six leaves.

stomatal closure, which subsequently decreased the transpiration rate (Figure 4G) and led to a variety of physiological changes, including drought tolerance (Figure 4B), Ca^{2+} underaccumulation (Figure 1A), and, hence, sensitivity to Ca^{2+} starvation (Figures 5E to 5H).

CAU1 Mediates *CAS* Expression by H4R3sme2 Methylation in the Promoter Region of *CAS*

CAU1 is the *Arabidopsis thaliana* homolog of PRMT5, a mammalian methyltransferase marking histone H4 Arg 3 with symmetric dimethylation (H4R3sme2) (Pollack et al., 1999; Bedford and Richard, 2005; Ancelin et al., 2006). To determine whether CAU1 regulates *CAS* expression via a similar mechanism, we performed a chromatin immunoprecipitation quantitative PCR (ChIP-qPCR) assay to analyze the H4R3sme2 levels in the *CAS* promoter region, using the H4R3sme2 antibody (Figures 6A and 6B). Our results showed that the H4R3me2 level in region B of the *CAS* promoter was significantly reduced in *cau1* (Figures 6A and 6B), suggesting that CAU1 regulates *CAS* transcription through histone methylation.

A ChIP-qPCR assay using a green fluorescent protein (GFP) antibody was also performed to determine whether CAU1 binds to the *CAS* chromatin (Figures 6A and 6C). CAU1 strongly associated with region A of the *CAS* promoter, whereas a similar CAU1-*CAS* interaction was not detected in regions B, C, and E, indicating that CAU1 binds to the *CAS* chromatin in region A and functions to mediate histone methylation levels in region B (Figure 6B).

Given that *CAS* expression was upregulated in response to elevated $[Ca^{2+}]_o$ (Figure 3A), we then determined the correlation between $[Ca^{2+}]_o$ and H4R3sme2 methylation in the *CAS* promoter. As shown in Figure 6D, elevated $[Ca^{2+}]_o$ significantly decreased the H4R3sme2 levels in region B of the *CAS* promoter from the wild type, while no change was observed in the *cau1* mutant. Further analysis showed that the binding of CAU1 to the *CAS* promoter (Figure 6E) as well as CAU1 protein levels decreased significantly in response to elevated $[Ca^{2+}]_o$ (Figure 6F). These data suggest that increased $[Ca^{2+}]_o$ decreases CAU1 protein levels and its binding to the *CAS* promoter, thus decreasing H4R3sme2 methylation of the *CAS* chromatin and enhancing the expression of *CAS*.

CAU1 Mediates the Expression of Genes Involved in Ca^{2+} Signaling and Homeostasis

PRMT5/SKB1/CAU1 has been proposed to mediate flowering time, the circadian clock or salt stress by histone methylation, and/or nonhistone methylation mechanisms; the nonhistone modification mechanism causes further modifications of mRNA splicing (Deng et al., 2010; Hong et al., 2010; Sanchez et al., 2010; Zhang et al., 2011). To test whether a pre-mRNA splicing mechanism was involved in the CAU1-regulated $[Ca^{2+}]_o$ signaling, we examined the transcripts of key genes in the CAS-IP3 pathway (Han et al., 2003; Tang et al., 2007). We failed to detect any alternatively spliced transcripts by both RT-PCR amplification and sequencing, even though some of these genes were previously predicted to have alternative splicing, and we performed

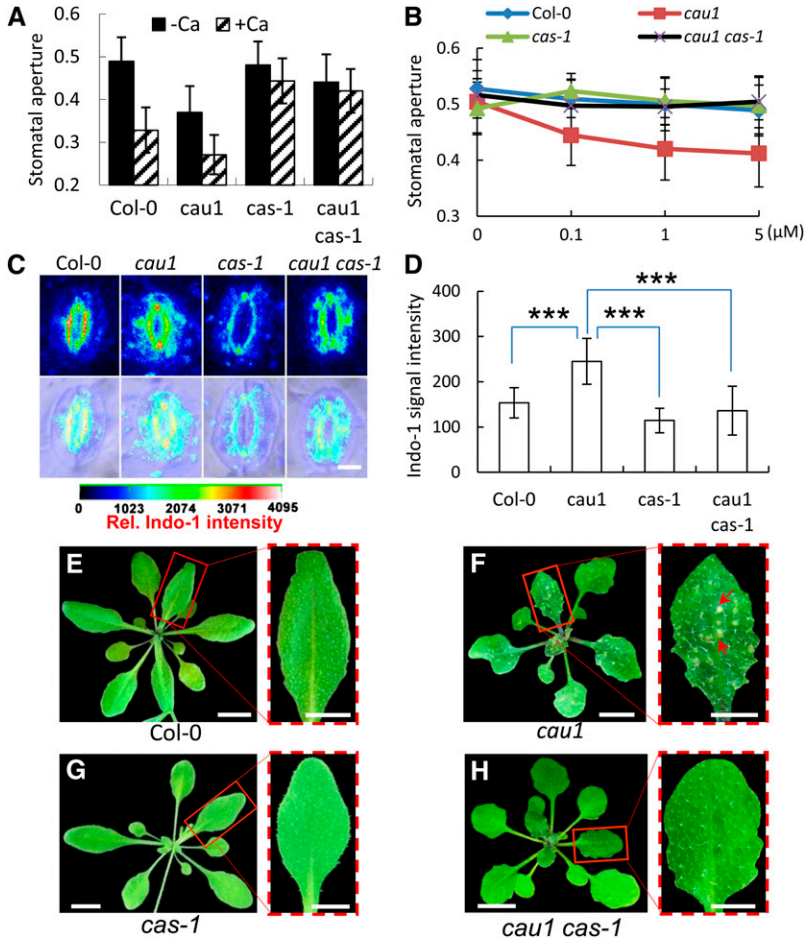

Figure 5. *CAU1* Regulates Guard Cell $[Ca^{2+}]_o$ Signaling and Ca^{2+} Starvation Tolerance via *CAS*.

(A) and **(B)** $[Ca^{2+}]_o$-induced stomatal closure in plants. As described in Methods, 2 mM Ca^{2+} **(A)** or a final concentration of 0, 0.1, 1, or 5 μM Ca^{2+} **(B)** was added, and stomatal aperture was calculated as the ratio of pore width/length. $n > 120$ stomata per Ca^{2+} treatment, and values are mean ± SD.
(C) Representative imaging of $[Ca^{2+}]_{cyt}$ in stomata of the wild type, *cau1*, *cas-1*, and double mutant *cau1 cas-1* by Indo-1 staining and UV confocal assay. The first row shows fluorescence images, and the second row shows merged fluorescence and bright-field images. $[Ca^{2+}]_{cyt}$ was calibrated and pseudo-color-coded according to the color scale shown.
(D) Quantification of the relative Indo-1 fluorescence intensities indicating $[Ca^{2+}]_{cyt}$ levels in stomata of the wild type, *cau1*, *cas-1*, and *cau1 cas-1*. Values are mean ± SD, $n = 46$. ***$P < 0.001$ in *t* tests.
(E) to **(H)** Chlorotic lesions in leaves of the wild type **(E)**, *cau1* **(F)**, *cas-1* **(G)**, and *cau1 cas-1* **(H)** exposed to calcium starvation. Each red dash-framed panel represents a scale-up of one corresponding leaf from **(E)** to **(H)**.
Bars = 5 μM in **(C)**, 1 cm in **(E)** to **(H)**, and 0.5 cm in the dash-framed panels.

RT-PCR using specifically designed primers for them (Deng et al., 2010; see Supplemental Figure 6 online).

Instead, the expression levels of several genes were significantly altered in *cau1*. Expression of *PLC3* and *PLC4*, two essential genes mediating IP3 production, markedly increased in *cau1* compared with the wild-type Col-0 (Figure 7A), while it decreased in *cas-1* and *cau1 cas-1* mutant plants (Figure 7B), supporting a model wherein CAU1 functions upstream of the CAS-IP3 cascade (Figure 8). *CAX1* and *CAX3*, which encode tonoplast-localized Ca^{2+} transporters, also showed higher expression levels in *cau1* (Figure 7A), though the upregulation was not affected by *CAS* (Figure 7B). Given that the overall Ca^{2+} content decreased in *cau1* shoots (Figure 1A; see Supplemental Figure 1A online), while the cytosolic Ca^{2+} concentration was increased (Figures 5C and 5D), we assume that the enhanced expression of *CAX1* and *CAX3* might merely be a local response to the increased requirement to move excess $[Ca^{2+}]_{cyt}$ to vacuoles. This assumption helps to explain the observations that less Ca^{2+} accumulated in *cau1* and *cax1/cax3* shoots (Figure 1A; see Supplemental Figure 1A online; Cheng et al., 2005; Conn et al., 2011). Note that we do not exclude the possibility that *CAX1* and *CAX3* may be actively involved in the $[Ca^{2+}]_o$ signaling pathway via complex mechanisms such as reported recently (Cho et al., 2012).

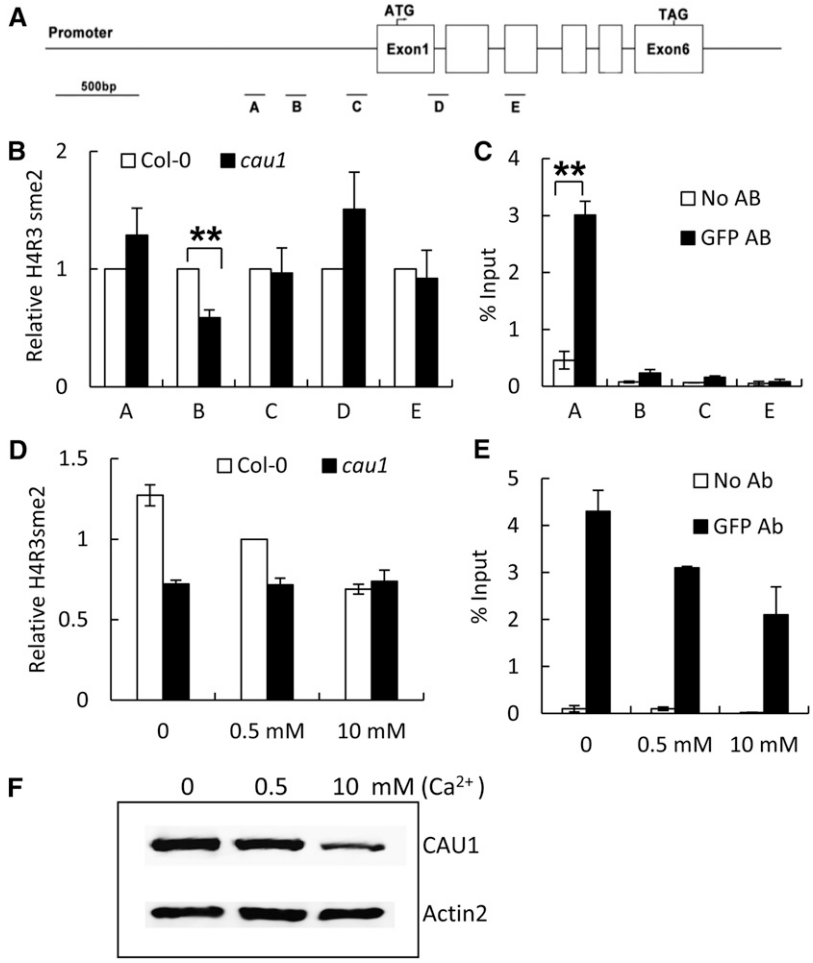

Figure 6. CAU1 Regulates the Histone Methylation of the *CAS* Chromatin and the Consequent *CAS* Expression in Response to $[Ca^{2+}]_o$.

(A) A diagram of the genomic structure of *CAS*. Genomic regions A to E subjected to ChIP assay are indicated.

(B) and **(C)** ChIP assay with antibodies against H4R3sme2 **(B)** to determine histone methylation status or against GFP **(C)** to determine if CAU1 binds to the *CAS* promoter using *35S/EYFP:CAU1-cau1* plants. *TUB8* was used as an internal control in **(B)**. Three independent experiments were performed, and values are mean ± SE.

(D) and **(E)** ChIP assay with antibodies against H4R3sme2 within the B region **(D)** or against GFP within the A region **(E)** of *CAS*. Wild-type and *cau1* plants were treated with calcium as indicated. Three independent experiments were performed, and *TUB8* was used as an internal control in **(D)**. Values are mean ± SE.

(F) Immunoblotting analysis of CAU1 levels in response to $[Ca^{2+}]_o$. Twenty-four-day-old plants were exposed to 0, 0.5, or 10 mM Ca^{2+} treatment for 4 d. Immunoblotting was performed as described in Methods. **$P < 0.01$.

cau1 Is Oversensitive to Abscisic Acid

Abscisic acid (ABA) is an essential plant hormone regulating $[Ca^{2+}]_{cyt}$ oscillations and the derived stomatal closure. Interestingly, we found that *cau1* was oversensitive to ABA in both seed germination and stomatal closure, and crossing *cas-1* to *cau1* fully or partially restored these phenotypes observed in *cau1* (see Supplemental Figure 7 online), which appear to indicate that in addition to $[Ca^{2+}]_o$, the CAU1–CAS interaction also responds to ABA. However, further analysis did not reveal significant differences in stomatal closure or seed germination between *cas-1* and the wild-type Col-0 (see Supplemental Figure 7 online). Taken together, these results suggest that ABA interacts with CAU1 to mediate stomatal closure, whereas the role of *CAS* in this process remains to be determined.

DISCUSSION

Elevations in $[Ca^{2+}]_o$ stimulate stomatal closure; however, the mechanism involved in $[Ca^{2+}]_o$ signal sensing and transduction remains elusive. In this study, we demonstrated that CAU1/PRMT5/SKB1, an H4R3sme2-type histone methylase, mediates $[Ca^{2+}]_o$ signaling by histone methylation of the *CAS* chromatin. Functional disruption of CAU1 led to steady upregulation of *CAS* and, consequently, enhanced stomatal closure and drought tolerance,

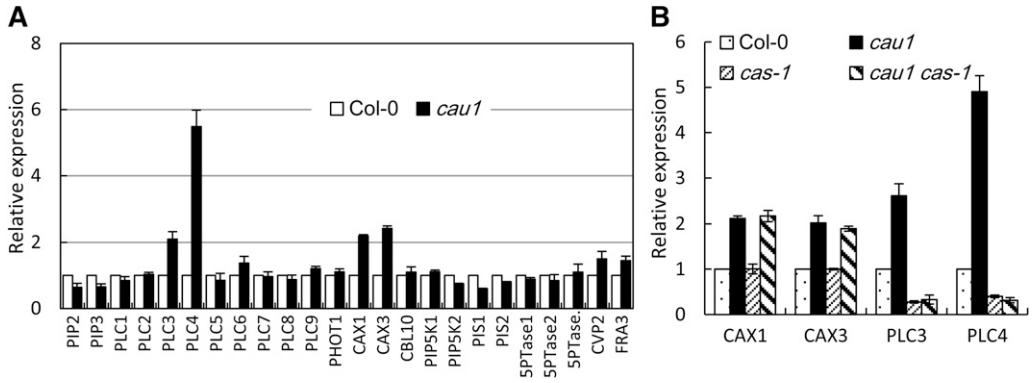

Figure 7. Analysis of Expression Levels of Ca^{2+} Homeostasis or Signaling Pathway Genes.

(A) Quantitative determination of expression levels of genes involved in the IP3 pathway or Ca^{2+} homeostasis.
(B) Expression of *CAX1*, *CAX3*, *PLC3*, and *PLC4* in *cau1*, *cas-1*, and *cau1 cas-1* plants. Plants were grown to 28 d old in soil.
The *y* axes show RNA levels normalized to those of *ACTIN2*. Values are mean ± SE, $n = 3$.

consistent with the model that CAU1 acts as an epigenetic repressor of *CAS* to mediate $[Ca^{2+}]_o$ signaling in stomatal closure.

CAU1 Is an Essential Component in $[Ca^{2+}]_o$ Signaling

It is known that $[Ca^{2+}]_o$ elicits intracellular $[Ca^{2+}]_{cyt}$ oscillations to close stomata (McAinsh et al., 1995; Allen et al., 2000, 2001), and CAS was proposed to be a $[Ca^{2+}]_o$ sensing receptor in this process to synchronize $[Ca^{2+}]_o$ and $[Ca^{2+}]_{cyt}$ oscillations (Han et al., 2003; Tang et al., 2007). Further research suggested that the IP3 cascade functions downstream of *CAS* in the $[Ca^{2+}]_o$ signaling pathway (Tang et al., 2007). Together, these discoveries imply that the $[Ca^{2+}]_o$ signaling mechanism might be highly conserved in plants and animals. However, the accuracy of this hypothesis remains an open question, mainly because CAS is exclusively localized to chloroplasts instead of the cell surface (Nomura et al., 2008; Vainonen et al., 2008; Weinl et al., 2008). This leaves a wide gap to be filled before it can be determined whether $[Ca^{2+}]_o$ serves as an extracellular first messenger in plant cells as previously proposed (Han et al., 2003; Tang et al., 2007) or acts in conjunction with other molecular machineries.

In a large-scale screening of Ca^{2+} accumulation mutants, we unexpectedly found that the histone methylase CAU1 functions as an upstream suppressor of *CAS* to mediate $[Ca^{2+}]_o$ sensing in guard cells (Figures 3 to 6 and 8). In response to $[Ca^{2+}]_o$ signals, both the protein levels of CAU1 and its association with *CAS* chromatin are reduced, consequently reducing histone methylation in the promoter region of *CAS* and, hence, derepressing *CAS* expression. The promoted *CAS* expression can then initiate intracellular Ca^{2+} signaling, leading to stomatal closure, which in return decreases the transpiration rate and Ca^{2+} translocation to the aerial parts. This model (Figure 8) fits well with the observations that the loss-of-function mutant *cau1* shows constantly high expression levels of *CAS*, a decreased transpiration rate and Ca^{2+} underaccumulation in leaves, as well as enhanced drought tolerance compared with the wild-type controls.

CAU1 was identified as SKB1/PRMT5 in previous work, where CAU1/SKB1/PRMT5 was found to act as an upstream suppressor of either *FLC* to mediate flowering time (Wang et al., 2007; Pei et al., 2007; Schmitz et al., 2008; Deng et al., 2010), or regulators other than *FLC* to mediate salt tolerance (Zhang et al., 2011), or the circadian clock (Hong et al., 2010; Sanchez et al., 2010). These observations suggest that CAU1 functions pleiotropically but mediates different biological processes via specific downstream target gene(s). Consistent with this postulation, our data demonstrated that CAU1 serves as an essential player in the $[Ca^{2+}]_o$-mediated stomatal closure and drought tolerance via its interaction with *CAS*. Furthermore, our data suggest that this process might at least be independent of plant development or flowering transition, as *cau1 cas-1* behaved similarly to *cau1* except for the stomatal closure and drought tolerance.

Although CAU1 mediates $[Ca^{2+}]_o$ signaling by the epigenetic modulation of *CAS* expression, it is probably not a direct extracellular Ca^{2+} sensor because of the following considerations: (1) CAU1/PRMT5 localizes to either the nucleus or the cytoplasm (Hong et al., 2010) rather than the cell surface, where $[Ca^{2+}]_o$ sensing occurs; and (2) the EF-hand domain for Ca^{2+} binding is not observed in CAU1. We therefore hypothesize that additional components might act upstream of CAU1 and CAS in the $[Ca^{2+}]_o$ signaling pathway. Furthermore, CAU1 also interacts with ABA to mediate stomatal closure (see Supplemental Figure 7 online), implying a potentially more complex role of CAU1 in *Arabidopsis* Ca^{2+} signaling.

CAU1 Mediates $[Ca^{2+}]_o$ Signaling Preferentially via Histone Modification of Its Downstream Target *CAS*

CAU1/PRMT5/SKB1 was shown to encode a histone methylase, though its effects on target genes are mediated by histone methylation, pre-mRNA splicing, or a combination of both (Pei et al., 2007; Wang et al., 2007; Schmitz et al., 2008; Deng et al., 2010; Hong et al., 2010; Sanchez et al., 2010; Zhang et al., 2011). In this study, however, we did not detect any alternative transcripts of *CAS* (see Supplemental Figure 6 online). By contrast, a significant increase in *CAS* mRNA was observed in *cau1* (Figure 3), consistent with the fact that under elevated $[Ca^{2+}]_o$

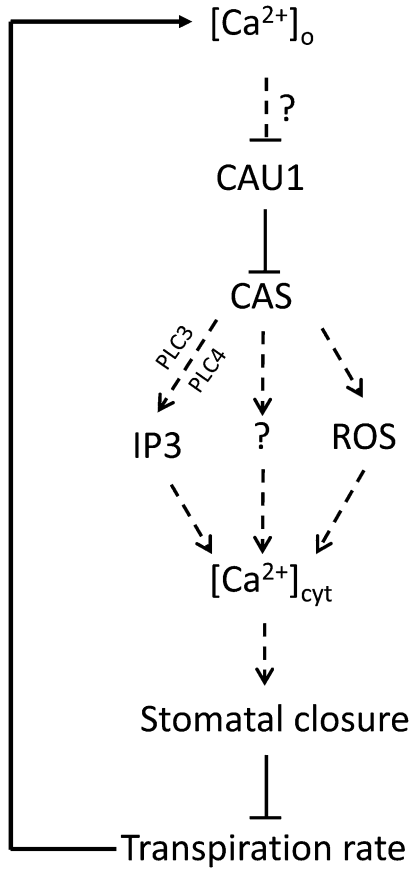

Figure 8. A Model for CAU1/CAS-Mediated $[Ca^{2+}]_o$ Signaling in Stomatal Closure.

Elevated $[Ca^{2+}]_o$ reduces the CAU1 association with the *CAS* promoter, which consequently decreases histone methylation of the *CAS* chromatin and lifts the repression of *CAS*. The resulting upregulation of *CAS* further evokes cytosolic Ca^{2+} ($[Ca^{2+}]_{cyt}$) and the subsequent stomatal closure (Tang et al., 2007), possibly through IP3 (Tang et al., 2007), ROS (Wang et al., 2012a), or mechanisms that are yet to be identified. Stomatal closure decreases the transpiration rate, leading to feedback inhibition of Ca^{2+} translocation to the plant aerial parts. Thus, a dynamic synchronization between $[Ca^{2+}]_o$ and stomatal closure is established and functions to mediate plant adaptation to the environment. The question marks and dashed lines represent possible unidentified steps or steps that have been identified but are not shown here.

treatments, histone methylation was significantly decreased in *CAS* chromatin (Figure 6).

Given that CAU1/SKB1/PRMT5 methylates the small nuclear ribonucleoprotein LSM4, thus regulating pre-mRNA splicing of a group of stress-related genes (Zhang et al., 2011), we then analyzed transcripts of additional genes believed to be involved in $[Ca^{2+}]_o$ signaling and intracellular Ca^{2+} homeostasis. We could not detect any alternative transcripts of these genes in the *cau1* mutant but observed an increase in *PLC3* and *PLC4* (Figure 7A), suggesting that CAU1 might mediate $[Ca^{2+}]_o$ sensing primarily through histone modification of the *CAS* chromatin. However, we do not exclude the possibility that alternative splicing mechanisms might also be involved because *CBL1*, which has been implicated in guard cell function (Kim et al., 2010), appeared to show alternative splicing affected by CAU1/PRMT5/SKB1 (Zhang et al., 2011).

Possible Downstream Regulatory Mechanisms in the CAU1-CAS–Mediated $[Ca^{2+}]_o$ Signaling in Stomatal Closure

It is generally believed that $[Ca^{2+}]_o$ mediates stomatal closure by evoking $[Ca^{2+}]_{cyt}$ (McAinsh et al., 1995; Allen et al., 2000, 2001), and CAS is required to synchronize $[Ca^{2+}]_o$ and $[Ca^{2+}]_{cyt}$ oscillations despite its subcellular localization to chloroplasts (Han et al., 2003; Tang et al., 2007; Nomura et al., 2008; Weinl et al., 2008). In agreement with these observations, our study showed that in *cau1*, *CAS* expression positively correlated with $[Ca^{2+}]_{cyt}$ levels and that the functional disruption of CAS significantly decreased the $[Ca^{2+}]_{cyt}$ levels (Figures 5C and 5D), supporting the model that the $[Ca^{2+}]_o$ signal is transduced and encoded in $[Ca^{2+}]_{cyt}$ oscillations through the interaction of CAU1 with *CAS* (Figure 8), though it remains to be determined how exactly CAU1-CAS translates the signal to $[Ca^{2+}]_{cyt}$ oscillation.

IP3 may act downstream of CAU1-CAS (Figure 8). In animal cells, it is well established that a $[Ca^{2+}]_o$ signal is perceived by the extracellular calcium receptor CaR and then transduced to the downstream IP3/Ca^{2+} cascade to modulate $[Ca^{2+}]_{cyt}$ (Brown et al., 1987, 1993; Shoback et al., 1988; Hofer 2005). The $[Ca^{2+}]_o$-induced IP3 generation was observed in plant guard cells in a *CAS*-dependent manner, and inhibition of IP3 synthesis resulted in failure to evoke $[Ca^{2+}]_{cyt}$ oscillations (Tang et al., 2007). Consistent with these findings, our research also found that the expression of *PLC3* and *PLC4*, two essential genes in regulating IP3 biosynthesis, showed a significant increase in *cau1* compared with the wild type (Figure 7A), and this increase was dependent on *CAS* (Figure 7B).

An alternative model may involve reactive oxygen species (ROS) signaling (Figure 8). H_2O_2 has been shown to elicit $[Ca^{2+}]_{cyt}$ (Allen et al., 2000; Pei et al., 2000). In a more recent study, a correlation between H_2O_2/NO and *CAS* was established; H_2O_2 and NO accumulation were observed in guard cells exposed to $[Ca^{2+}]_o$, and the production of H_2O_2 and NO were dependent on *CAS*. More importantly, stomatal closure in the functional disruption mutants *CASas* and *noa1* was insensitive to $[Ca^{2+}]_o$ treatments (Wang et al., 2012a). All these observations appear to support the hypothesis that the ROS pathway might act downstream of CAU1-CAS to mediate the $[Ca^{2+}]_o$ signaling in guard cells.

Additionally, other unknown mechanisms might also exist (Figure 8). The rationale for this hypothesis is that pre-mRNA splicing mediated by CAU1/SKB1/PRMT5 appears to be a common mechanism in regulating diverse biological processes (Deng et al., 2010; Hong et al., 2010; Sanchez et al., 2010; Zhang et al., 2011). However, we were not able to detect any alternative splicing in those genes already correlated to IP3/Ca^{2+} signaling or Ca^{2+} homeostasis (see Supplemental Figure 6 online). This may be simply due to the fact that unknown genes that are yet to be associated with this pathway exist, an idea that is supported by the observation that *CBL1* showed altered transcript splicing in *skb1* (Zhang et al., 2011).

In summary, the functional characterization of CAU1 revealed that CAU1/PRMT5/SKB1 serves as an epigenetic suppressor of *CAS* and hence plays an essential role in $[Ca^{2+}]_o$ signaling in guard cells to mediate stomatal closure and the consequent drought tolerance.

METHODS

Plant Materials, Growth Conditions, and Physiological Analyses

Arabidopsis thaliana plants were grown in soil to the indicated ages at 22°C with 16-h-light/8-h-dark cycles. At 14 d of age, drought stress was induced by withholding watering for 9 to 14 d, and the survival rate was scored 7 d after reirrigation. Alternatively, as indicated, rosette leaves of 22-d-old plants were collected, and their fresh weights were used as a measure at indicated time points to determine the water loss rate (Vartanian et al., 1994; Pei et al., 1998). Stomatal assays were performed as previously described for the 2 mM Ca^{2+} treatment (Pei et al., 2000) or with minor modifications; the abaxial epidermis was peeled from rosette leaves of 22-d-old plants to determine stomatal aperture by direct imaging. When indicated, the epidermal peels were put in an EGTA-containing buffer (10 mM KCl, 6 mM EGTA, and 10 mM MES-Tris, pH 6.15) and incubated under light conditions for 2 h to allow the stomata to open. Subsequently, the epidermal peels were transferred to the same buffer supplemented with 32.68 μM, 340 μM, or 1.3 mM $CaCl_2$, corresponding to 0.1, 1, or 5 μM free Ca^{2+} according to Maxchelator (http://www.stanford.edu/~cpatton/webmaxc/webmaxcS.htm), and incubated under light conditions for 2 h. Stomatal apertures were determined by measuring the pore widths and lengths with a digital ruler in Image-pro plus 6.0 (Media Cybernetics).

Alternatively, plants were grown in quarter-strength hydroponics as previously described (Arteca and Arteca, 2000; Gong et al., 2003). At ~3 weeks of age, plants were treated with or without 0.5 or 10 mM Ca^{2+} for 4 d. Rosette leaves and roots were sampled and subjected to further analyses as indicated.

The *skb1-2* mutant was ordered from the SALK T-DNA collection (Salk_095085) from the ABRC. Isolation of ion accumulation mutants was performed according to the previously described screen at the University of California at San Diego (Lahner et al., 2003), with minor modification: fast neutron-mutagenized M_2 seeds (population M_2F-02-01; Lehle Seeds) were planted in peat moss soil (Pindstrup) premixed with 5 PPM of aluminum, calcium, iron, potassium, manganese, lead, and zinc. Mature dried cauline leaves were sampled and subjected to inductively coupled plasma-mass spectrometry (ICP-MS) analysis of ion accumulation as indicated.

Map-Based Cloning, Sequencing, and Genetic Complementation Assay

The Ca^{2+} underaccumulation mutant *cau1* in Col-0 background was crossed to the ecotype Landsberg *erecta* to generate a mapping population. SSLP markers were designed according to The Arabidopsis Information Resource (http://www.Arabidopsis.org). Bulked segregant analysis was performed to determine the genetic linkage between *cau1* and SSLP markers (Michelmore et al., 1991). Fine mapping of *cau1* was performed using DNA from 5742 F2 mutants as previously described (Lukowitz et al., 2000). Mutations in *CAU1* were determined by PCR amplification and sequencing using *CAU1-1* primers (see Supplemental Table 2 online).

For the complementation of *cau1*, direct transformation of *CAU1*-containing constructs into *cau1* was not used because *cau1* is hypersensitive to bacteria. Instead, transgenic plants harboring 35S/*CAU1*-pBI121 or 35S/*EYFP*:*CAU1*-pMON530 were crossed to the *cau1* mutant. The derived F2 progenies were then screened for kanamycin resistance, and *cau1* homozygous plants were determined by PCR amplification and sequencing using *CAU1-2* primers (see Supplemental Table 2 online).

DNA Constructs and Plant Transformation

The *CAU1* cDNA was amplified by RT-PCR. The two restriction sites for *Bam*HI and *Sac*I were introduced using *CAU1-3* primers; *Xho*I and *Eco*RI sites were introduced using *CAU1-4* primers (primers are listed in Supplemental Table 2 online). The resulting fragments were confirmed by sequencing and then subcloned into the binary vector pBI121 (predigested with *Bam*HI and *Sac*I) or 35S/*EYFP*-pMON530 (predigested with *Xho*I and *Eco*RI). The generated constructs 35S/*CAU1*-pBI121 and 35S/*EYFP*:*CAU1*-pMON530, together with the construct 35S/*EYFP*-pMON530, were transformed into Col-0 by floral dip (Clough and Bent, 1998). Transgenic lines with a segregation rate of 3:1 grown on kanamycin plates were used for further homozygote and strong allele screenings.

Microarray Analysis

Total RNA was isolated from rosette leaves of 4-week-old Col-0 and *cau1* mutant plants using TRIzol reagent (Invitrogen). Microarray hybridization to the *Arabidopsis* whole-genome ATH1 arrays was performed by Shanghai OE Biotech. Data were extracted and normalized according to the manufacturer's standard protocol.

RT-PCR/Quantitative RT-PCR

Total RNA from plants grown under the indicated conditions was isolated using TRIzol reagent. First-strand cDNA synthesis, RT-PCR, and quantitative RT-PCR were performed as previously described (Li et al., 2010). *CAU1-5*, *CAS-RT*, and *Actin2* primers were used in regular RT-PCR. *CAS-QP* and *Actin2-QP* primers were used in quantitative RT-PCR (see Supplemental Table 2 online).

Histochemical Analysis

Transgenic plants expressing the construct *pCAS*/*GUS*-pBI101 (Han et al., 2003) were crossed to *cau1* mutant plants. Plants showing the *cau1* phenotype in the F2 population were subjected to histochemical analysis as previously described (Li et al., 2010).

Isolation of *cas-1* and *cau1 cas-1* Mutant Plants and Introduction of 35S/*CAU1*-pBI121 into *cau1*

The T-DNA insertion line SALK_070416 obtained from the ABRC was screened for the homozygous knockout mutant *cas-1* as previously described (Weinl et al., 2008). To generate the *cau1 cas-1* double mutant, *cau1* was crossed to *cas-1* to make an F2 population; *cau1*-like plants were further analyzed to isolate the genotype *cas-1*/*cas-1* using the PCR primers *CAS*-salk and LBa1 as previously described (Krysan et al., 1999). The same strategy was used to introduce the construct 35S/*CAU1*-pBI121 into *cau1*: Col-0 plants containing 35S/*CAU1*-pBI121 were crossed to *cau1*, and further PCR analysis was performed using primers mentioned above for homozygosity screening.

$[Ca^{2+}]_{cyt}$ Imaging in Guard Cells

Fluorescence imaging of $[Ca^{2+}]_{cyt}$ was performed according to Legué et al. (1997) and Wymer et al. (1997) with minor modifications: Abaxial epidermis peels taken from 22-d-old soil-grown plants were perfused with 20 μM Indo-1 solution (in 10 mM dimethylglutaric acid, pH 4.5) and incubated in the dark for 1 h. Then, the peels were washed with liquid

Murashige and Skoog medium followed by imaging using confocal laser scanning microscopy (Carl Zeiss; LSM 510 Meta) (364-nm excitation and 400- to 435-nm and 480 ± 20-nm emission). Calcium levels were calculated and pseudocolored according to the color scale as described (Wang et al., 2012b). Briefly, pseudocolor ratio images of calcium level were calculated with the Olympus Fluoview ver. 1.7a viewer tool (Olympus) to measure fluorescence intensities. White color indicates ~2 times the calcium level of that indicated by blue color and 1.5 times of that indicated by yellow color.

Chromatin Immunoprecipitation Assay

Twenty-day-old Col-0, *cau1*, and 35S/*EYFP*:*CAU1-cau1* plants grown under long-day conditions were harvested for the ChIP assay (Aggarwal et al., 2010). Total proteins extracted from plants of Col-0 and *cau1* were immunoprecipitated with antisymmetric dimethyl-H4R3 antibody (Abcam), and proteins from *cau1* and 35S/*EYFP*:*CAU1-cau1* were immunoprecipitated with an anti-GFP antibody (Invitrogen). Primers used for ChIP-qPCR are as follows: region A (*CAS-9*), region B (*CAS-11*), region C (*CAS-14*), region D (*CAS-17*), and region E (*CAS-19*). *TUB8* was used as a control (Mathieu et al., 2005). The primer sequences are given in Supplemental Table 2 online.

Protein Gel Blotting Analysis

Transgenic 35S/*EYFP*:*CAU1-cau1* plants were grown in hydroponics to 24 d of age and then exposed to Ca^{2+} treatments at the indicated concentrations for 4 d. Total protein were extracted from leaf samples using buffer E (125 mM Tris-HCl, pH 8.0, 1% [w/v] SDS, 10% [v/v] glycerol, and 50 mM NaS_2O_5). Thirty micrograms of total proteins of each sample were separated on 12% SDS-PAGE gel and analyzed by protein gel blot according to the manufacturer's instructions. Mouse anti-Actin2 and -GFP (Abmart; at 1:5000 dilution) were used as primary antibodies. The membranes were visualized using a Super-Signal West Pico Chemiluminescent Substrate Kit (Thermo Scientific) according to the manufacturer's instructions.

Statistical Analysis

Two-tailed Student's *t* tests were performed. Differences were deemed significant at $P < 0.05$ and extremely significant at $P < 0.01$.

Accession Numbers

Sequence data from this article can be found in the Arabidopsis Genome Initiative or GenBank/EMBL databases under the following accession numbers: CAU1 (At4g31120), CAS (At5g23060), CAX1 (At2g38170), CAX3 (At3g51860), PLC3 (At5g58670), PLC4 (At5g58670), and Actin2 (At3g18780). Additional sequence data are available in Supplemental Table 1 online.

Supplemental Data

The following materials are available in the online version of this article.

Supplemental Figure 1. CAU1 Affects Calcium Accumulation.

Supplemental Figure 2. *cau1* Mutant Shows Pleiotropic Phenotypes.

Supplemental Figure 3. Complementation Assay of the *cau1* Mutant.

Supplemental Figure 4. Stomatal Closure, Drought Tolerance, and *CAS* Expression in 35S/*CAU1-cau1*.

Supplemental Figure 5. *CAU1* Complements Stomatal Closure and $[Ca^{2+}]_o$ Signaling Phenotype in the *cau1* Mutant.

Supplemental Figure 6. Analysis of Alternative Splicing of Ca^{2+} Homeostasis or Signaling Pathway Genes.

Supplemental Figure 7. *cau1* Is Hypersensitive to ABA.

Supplemental Table 1. Transcriptomic Analysis of Ca^{2+} Homeostasis Genes, Ca^{2+} Signaling Pathway Genes, and Genes Known to Be Regulated by CAU1.

Supplemental Table 2. List of Primer Sequences.

ACKNOWLEDGMENTS

We thank Zhenming Pei (Duke University) for kindly providing the seeds of *pCAS/GUS*; Julian Schroeder (University of California at San Diego), Xiao-Feng Cao (Chinese Academy of Sciences), and Hai Huang (Chinese Academy of Sciences) for helpful discussion; Zhenbiao Yang and Irene Lavagi (University of California at Riverside) for careful reading of the article; and Xiao-Shu Gao (Shanghai Institutes for Biological Sciences) for helping with confocal microscopy. This research was supported by the National Science Foundation of China (30900785 and 31121063), the Chinese Academy of Sciences/State Administration of Foreign Experts Affairs International Partnership Program for Creative Research Teams, the Chinese Academy of Sciences program for Creative Basic Research (KSCX2-EW-J-12), and in part by the Sanofi-Aventis-Shanghai Institutes for Biological Sciences Scholarship Program.

AUTHOR CONTRIBUTIONS

J.-M.G. and Y.-L.F. designed the research. Y.-L.F., G.-B.Z., X.-F.L., Y.G., and H-Y.Y. performed the research. J.-M.G. and Y.-L.F. analyzed the data and wrote the article.

Received May 20, 2013; revised July 1, 2013; accepted July 30, 2013; published August 13, 2013.

REFERENCES

Aggarwal, P., Vaites, L.P., Kim, J.K., Mellert, H., Gurung, B., Nakagawa, H., Herlyn, M., Hua, X., Rustgi, A.K., McMahon, S.B., and Diehl, J.A. (2010). Nuclear cyclin D1/CDK4 kinase regulates CUL4 expression and triggers neoplastic growth via activation of the PRMT5 methyltransferase. Cancer Cell **18:** 329–340.

Allen, G.J., Chu, S.P., Harrington, C.L., Schumacher, K., Hoffmann, T., Tang, Y.Y., Grill, E., and Schroeder, J.I. (2001). A defined range of guard cell calcium oscillation parameters encodes stomatal movements. Nature **411:** 1053–1057.

Allen, G.J., Chu, S.P., Schumacher, K., Shimazaki, C.T., Vafeados, D., Kemper, A., Hawke, S.D., Tallman, G., Tsien, R.Y., Harper, J.F., Chory, J., and Schroeder, J.I. (2000). Alteration of stimulus-specific guard cell calcium oscillations and stomatal closing in *Arabidopsis det3* mutant. Science **289:** 2338–2342.

Ancelin, K., Lange, U.C., Hajkova, P., Schneider, R., Bannister, A.J., Kouzarides, T., and Surani, M.A. (2006). Blimp1 associates with Prmt5 and directs histone arginine methylation in mouse germ cells. Nat. Cell Biol. **8:** 623–630.

Arteca, R.N., and Arteca, J.M. (2000). A novel method for growing *Arabidopsis thaliana* plants hydroponically. Physiol. Plant. **108:** 188–193.

Bedford, M.T., and Richard, S. (2005). Arginine methylation an emerging regulator of protein function. Mol. Cell **18:** 263–272.

Brown, E., Enyedi, P., LeBoff, M., Rotberg, J., Preston, J., and Chen, C. (1987). High extracellular Ca^{2+} and Mg^{2+} stimulate accumulation

of inositol phosphates in bovine parathyroid cells. FEBS Lett. **218:** 113–118.

Brown, E.M. (1991). Extracellular Ca^{2+} sensing, regulation of parathyroid cell function, and role of Ca^{2+} and other ions as extracellular (first) messengers. Physiol. Rev. **71:** 371–411.

Brown, E.M., Gamba, G., Riccardi, D., Lombardi, M., Butters, R., Kifor, O., Sun, A., Hediger, M.A., Lytton, J., and Hebert, S.C. (1993). Cloning and characterization of an extracellular $Ca^{(2+)}$-sensing receptor from bovine parathyroid. Nature **366:** 575–580.

Bush, D.S. (1995). Calcium regulation in plant cells and its role in signaling. Annu. Rev. Plant Physiol. Plant Mol. Biol. **46:** 95–122.

Cheng, N.H., Pittman, J.K., Shigaki, T., Lachmansingh, J., LeClere, S., Lahner, B., Salt, D.E., and Hirschi, K.D. (2005). Functional association of Arabidopsis CAX1 and CAX3 is required for normal growth and ion homeostasis. Plant Physiol. **138:** 2048–2060.

Cho, D., Villiers, F., Kroniewicz, L., Lee, S., Seo, Y.J., Hirschi, K.D., Leonhardt, N., and Kwak, J.M. (2012). Vacuolar CAX1 and CAX3 influence auxin transport in guard cells via regulation of apoplastic pH. Plant Physiol. **160:** 1293–1302.

Clough, S.J., and Bent, A.F. (1998). Floral dip: A simplified method for *Agrobacterium*-mediated transformation of *Arabidopsis thaliana*. Plant J. **16:** 735–743.

Conn, S.J., et al. (2011). Cell-specific vacuolar calcium storage mediated by CAX1 regulates apoplastic calcium concentration, gas exchange, and plant productivity in *Arabidopsis*. Plant Cell **23:** 240–257.

Deng, X., Gu, L., Liu, C., Lu, T., Lu, F., Lu, Z., Cui, P., Pei, Y., Wang, B., Hu, S., and Cao, X. (2010). Arginine methylation mediated by the *Arabidopsis* homolog of PRMT5 is essential for proper pre-mRNA splicing. Proc. Natl. Acad. Sci. USA **107:** 19114–19119.

Gong, J.M., Lee, D.A., and Schroeder, J.I. (2003). Long-distance root-to-shoot transport of phytochelatins and cadmium in *Arabidopsis*. Proc. Natl. Acad. Sci. USA **100:** 10118–10123.

Han, S., Tang, R., Anderson, L.K., Woerner, T.E., and Pei, Z.M. (2003). A cell surface receptor mediates extracellular $Ca^{(2+)}$ sensing in guard cells. Nature **425:** 196–200.

Harper, J.F. (2001). Dissecting calcium oscillators in plant cells. Trends Plant Sci. **6:** 395–397.

Helpler, P.K., and Wayne, R.O. (1985). Calcium and plant development. Annu. Rev. Plant Physiol. **36:** 397–439.

Hetherington, A.M., and Brownlee, C. (2004). The generation of $Ca^{(2+)}$ signals in plants. Annu. Rev. Plant Biol. **55:** 401–427.

Hofer, A.M. (2005). Another dimension to calcium signaling: A look at extracellular calcium. J. Cell Sci. **118:** 855–862.

Hong, S., Song, H.R., Lutz, K., Kerstetter, R.A., Michael, T.P., and McClung, C.R. (2010). Type II protein arginine methyltransferase 5 (PRMT5) is required for circadian period determination in *Arabidopsis thaliana*. Proc. Natl. Acad. Sci. USA **107:** 21211–21216.

Kim, T.H., Böhmer, M., Hu, H., Nishimura, N., and Schroeder, J.I. (2010). Guard cell signal transduction network: advances in understanding abscisic acid, CO_2, and Ca^{2+} signaling. Annu. Rev. Plant Biol. **61:** 561–591.

Krysan, P.J., Young, J.C., and Sussman, M.R. (1999). T-DNA as an insertional mutagen in *Arabidopsis*. Plant Cell **11:** 2283–2290.

Lahner, B., Gong, J., Mahmoudian, M., Smith, E.L., Abid, K.B., Rogers, E.E., Guerinot, M.L., Harper, J.F., Ward, J.M., McIntyre, L., Schroeder, J.I., and Salt, D.E. (2003). Genomic scale profiling of nutrient and trace elements in *Arabidopsis thaliana*. Nat. Biotechnol. **21:** 1215–1221.

Legué, V., Blancaflor, E., Wymer, C., Perbal, G., Fantin, D., and Gilroy, S. (1997). Cytoplasmic free Ca^{2+} in Arabidopsis roots changes in response to touch but not gravity. Plant Physiol. **114:** 789–800.

Li, J.Y., et al. (2010). The *Arabidopsis* nitrate transporter NRT1.8 functions in nitrate removal from the xylem sap and mediates cadmium tolerance. Plant Cell **22:** 1633–1646.

Luan, S., Kudla, J., Rodriguez-Concepcion, M., Yalovsky, S., and Gruissem, W. (2002). Calmodulins and calcineurin B-like proteins: calcium sensors for specific signal response coupling in plants. Plant Cell **14** (suppl.)**:** S389–S400.

Lukowitz, W., Gillmor, C.S., and Scheible, W.R. (2000). Positional cloning in Arabidopsis. Why it feels good to have a genome initiative working for you. Plant Physiol. **123:** 795–805.

MacRobbie, E.A.C. (1992). Calcium and ABA-induced stomatal closure. Philos. Trans. R. Soc. Lond. B Biol. Sci. **338:** 5–18.

Mathieu, O., Probst, A.V., and Paszkowski, J. (2005). Distinct regulation of histone H3 methylation at lysines 27 and 9 by CpG methylation in *Arabidopsis*. EMBO J. **24:** 2783–2791.

McAinsh, M.R., Webb, A., Taylor, J.E., and Hetherington, A.M. (1995). Stimulus-induced oscillations in guard cell cytosolic free calcium. Plant Cell **7:** 1207–1219.

Michelmore, R.W., Paran, I., and Kesseli, R.V. (1991). Identification of markers linked to disease-resistance genes by bulked segregant analysis: A rapid method to detect markers in specific genomic regions by using segregating populations. Proc. Natl. Acad. Sci. USA **88:** 9828–9832.

Nomura, H., Komori, T., Kobori, M., Nakahira, Y., and Shiina, T. (2008). Evidence for chloroplast control of external Ca^{2+}-induced cytosolic Ca^{2+} transients and stomatal closure. Plant J. **53:** 988–998.

Pei, Y., Niu, L., Lu, F., Liu, C., Zhai, J., Kong, X., and Cao, X. (2007). Mutations in the Type II protein arginine methyltransferase AtPRMT5 result in pleiotropic developmental defects in Arabidopsis. Plant Physiol. **144:** 1913–1923.

Pei, Z.M., Ghassemian, M., Kwak, C.M., McCourt, P., and Schroeder, J.I. (1998). Role of farnesyltransferase in ABA regulation of guard cell anion channels and plant water loss. Science **282:** 287–290.

Pei, Z.M., Murata, Y., Benning, G., Thomine, S., Klüsener, B., Allen, G.J., Grill, E., and Schroeder, J.I. (2000). Calcium channels activated by hydrogen peroxide mediate abscisic acid signalling in guard cells. Nature **406:** 731–734.

Pollack, B.P., Kotenko, S.V., He, W., Izotova, L.S., Barnoski, B.L., and Pestka, S. (1999). The human homologue of the yeast proteins Skb1 and Hsl7p interacts with Jak kinases and contains protein methyltransferase activity. J. Biol. Chem. **274:** 31531–31542.

Poovaiah, B.W., and Reddy, A.S. (1993). Calcium and signal transduction in plants. CRC Crit. Rev. Plant Sci. **12:** 185–211.

Rudd, J.J., and Franklin-Tong, V.E. (1999). Calcium signaling in plants. Cell. Mol. Life Sci. **55:** 214–232.

Sanchez, S.E., et al. (2010). A methyl transferase links the circadian clock to the regulation of alternative splicing. Nature **468:** 112–116.

Sanders, D., Brownlee, C., and Harper, J.F. (1999). Communicating with calcium. Plant Cell **11:** 691–706.

Sanders, D., Pelloux, J., Brownlee, C., and Harper, J.F. (2002). Calcium at the crossroads of signaling. Plant Cell **14** (Suppl)**:** S401–S417.

Schmitz, R.J., Sung, S., and Amasino, R.M. (2008). Histone arginine methylation is required for vernalization-induced epigenetic silencing of FLC in winter-annual *Arabidopsis thaliana*. Proc. Natl. Acad. Sci. USA **105:** 411–416.

Schwartz, A. (1985). Role of Ca^{2+} and EGTA on stomatal movements in *Commelina communis L*. Plant Physiol. **79:** 1003–1005.

Shoback, D., Thatcher, J., Leombruno, R., and Brown, E. (1983). Effects of extracellular Ca^{++} and Mg^{++} on cytosolic Ca^{++} and PTH release in dispersed bovine parathyroid cells. Endocrinology **113:** 424–426.

Shoback, D.M., Membreno, L.A., and McGhee, J.G. (1988). High calcium and other divalent cations increase inositol trisphosphate in bovine parathyroid cells. Endocrinology **123:** 382–389.

Shoback, D.M., Thatcher, J.G., and Brown, E.M. (1984). Interaction of extracellular calcium and magnesium in the regulation of cytosolic calcium and PTH release in dispersed bovine parathyroid cells. Mol. Cell. Endocrinol. **38:** 179–186.

Tang, R.H., Han, S., Zheng, H., Cook, C.W., Choi, C.S., Woerner, T.E., Jackson, R.B., and Pei, Z.M. (2007). Coupling diurnal cytosolic Ca^{2+} oscillations to the CAS-IP_3 pathway in *Arabidopsis*. Science **315:** 1423–1426.

Thuleau, P., Schroeder, J.I., and Ranjeva, R. (1998). Recent advances in the regulation of plant calcium channels: Evidence for regulation by G-proteins, the cytoskeleton and second messengers. Curr. Opin. Plant Biol. **1:** 424–427.

Vainonen, J.P., Sakuragi, Y., Stael, S., Tikkanen, M., Allahverdiyeva, Y., Paakkarinen, V., Aro, E., Suorsa, M., Scheller, H.V., Vener, A.V., and Aro, E.M. (2008). Light regulation of CaS, a novel phosphoprotein in the thylakoid membrane of *Arabidopsis thaliana*. FEBS J. **275:** 1767–1777.

Vartanian, N., Marcotte, L., and Giraudat, J. (1994). Drought rhizogenesis in *Arabidopsis thaliana* (differential responses of hormonal mutants). Plant Physiol. **104:** 761–767.

Wang, W.H., Yi, X.Q., Han, A.D., Liu, T.W., Chen, J., Wu, F.H., Dong, X.J., He, J.X., Pei, Z.M., and Zheng, H.L. (2012a). Calcium-sensing receptor regulates stomatal closure through hydrogen peroxide and nitric oxide in response to extracellular calcium in *Arabidopsis*. J. Exp. Bot. **63:** 177–190.

Wang, X., Zhang, Y., Ma, Q., Zhang, Z., Xue, Y., Bao, S., and Chong, K. (2007). SKB1-mediated symmetric dimethylation of histone H4R3 controls flowering time in *Arabidopsis*. EMBO J. **26:** 1934–1941.

Wang, Y., Chu, Y.J., and Xue, H.W. (2012b). Inositol polyphosphate 5-phosphatase-controlled $Ins(1,4,5)P_3/Ca^{2+}$ is crucial for maintaining pollen dormancy and regulating early germination of pollen. Development **139:** 2221–2233.

Weinl, S., Held, K., Schlücking, K., Steinhorst, L., Kuhlgert, S., Hippler, M., and Kudla, J. (2008). A plastid protein crucial for Ca^{2+}-regulated stomatal responses. New Phytol. **179:** 675–686.

Wymer, C.L., Bibikova, T.N., and Gilroy, S. (1997). Cytoplasmic free calcium distributions during the development of root hairs of *Arabidopsis thaliana*. Plant J. **12:** 427–439.

Zhang, Z., et al. (2011). *Arabidopsis* floral initiator SKB1 confers high salt tolerance by regulating transcription and pre-mRNA splicing through altering histone H4R3 and small nuclear ribonucleoprotein LSM4 methylation. Plant Cell **23:** 396–411.

Zielinski, R.E. (1998). Calmodulin and calmodulin-binding proteins in plants. Annu. Rev. Plant Physiol. Plant Mol. Biol. **49:** 697–725.